# EFFECT OF ORIENTATION OF WORKPIECE AND FILTER CUT-OFFS IN THE SURFACE ROUGHNESS EVALUATION USING MACHINE VISION

*Srinagalakshmi NAMMI [1], Sree lakshmi UPPU [2] and Ramamoorthy B [3]*

*1 Research Scholar, #363, Sarayu hostel, IIT Madras, Chennai 600 036, India, snl.nammi@gmail.com*
*2 Bachelor's student, IIT Madras 3 Professor, Manufacturing Engineering section, IIT Madras.*

**Abstract**:

In this work, surface roughness of milled surfaces is quantified using digital images obtained by a machine vision system. Images captured are pre-processed for waviness profile elimination using digital filters. The influence of various filters at different cut-offs on the image based surface roughness value '$G_a$' is studied in comparison with the conventional surface roughness parameter, '$R_a$'.

In addition, Grey Level Co-occurrence Matrix (GLCM) is used to determine the image quantification parameters namely contrast, correlation, and energy using the images of machined components arranged in varying orientations in the horizontal plane. The effect of orientation of components on vision parameters is studied. Subsequent improvement in the value of vision roughness parameters obtained before and after the application of filters on these preprocessed digital images is established. All the results are compared with $R_a$ obtained using stylus method and analyzed for the scale, translation, rotation invariance of image based roughness.

**Keywords**: Surface roughness, Digital filters, Cut-off

## 1. INTRODUCTION

The measurement of roughness on machined surfaces is of great importance for manufacturing industries as the roughness of a surface has a considerable influence on its quality and function of products. The conventional method for measuring surface roughness is to pass a stylus probe across the surface and monitor its movement such that the surface micro profile can be traced. A common drawback of this approach is the 1-D trace instead of a 2-D surface region using which the roughness is evaluated at any one time. Also the transducer is very sensitive and the stylus tip is fragile. Another problem with the stylus measurement technique is the size of the stylus radius and the crevices of the surface. If the crevices are narrow such that the stylus cannot penetrate all the way to the bottom, the measurement will not be accurate. Considering these drawbacks the need and the importance for non-contact techniques for measurement of surface roughness becomes apparent.

In recent years, the advent of high-speed general-purpose digital computers and vision systems has made image analysis easier and more flexible. Computer vision techniques have been used for measuring surface roughness by many researchers [1]. Many pre-processing techniques such as shadow removal and illumination compensation have been employed to extract necessary features from the captured images in various applications [2]. In stylus measurement of surface roughness, analogue filtering is performed on the input signals to remove the waviness profile from the traced primary profile resulting in the roughness profile which is used for texture analysis [3]. In a similar fashion, digital filtering can be performed using machine vision approach on the images of the components before vision roughness is evaluated.

In addition, the term texture analysis is considered a basic issue in image processing and computer vision [4]. First-order texture features, extract data from the information provided by the intensity histograms, it yields no information about the locations of the pixels. The second-order texture features take into account the specific position of a pixel relative to another. The most popularly used second-order method is the grey level co-occurrence matrix (GLCM) method [5], which depends on constructing matrices by counting the number of occurrences of pixel pairs of given intensities at a given displacement.

The present study deals with the application of digital filters to captured images in machine vision technique to predict the surface roughness of a milled component and compare it to that of the stylus roughness value. The influence of component orientation on image quantification parameters derived based on GLCM has also been presented. The effect of image orientation on image quantification for the digital images of components captured by varying the component orientations was studied. This was tried out by applying gray level co-occurrence matrix (GLCM) based parameters. Statistical parameters are effective because they provide a good enhancement of the signal over the noise introduced into the system.

The earliest approach towards higher order statistics was developed by Haralick *et al* [6]. Co-occurrence matrix approach has been used for the calculation of various features based on the matrices and for the classification of images. Grey level co-occurrence matrix (GLCM) depends on constructing matrices by counting the number of occurrences of pixel pairs of given intensities at a given displacement. GLCM is one of the most known texture analysis methods, estimates image properties related to second-order statistics. Each entry $(i,j)$ in GLCM corresponds to the number of occurrences of the pair of grey levels $i$ and $j$ which are at distance $d$ apart in original image. Haralick [6] suggested a set 14 textural features which can be extracted from the GLCM matrices. These features contain information about image textural characteristics as homogeneity, grey tone linear dependencies (linear structure), contrast, number and nature of boundaries present and the complexity of image. The GLCM has been widely used for texture analysis in many applications. Gadelmawla [7] introduced vision system to capture images for surfaces to be characterized and developed software to analyze the captured images based on the GLCM. A new parameter called maximum width of the matrix was introduced which can be used as an indicator for surface roughness.

Roughness is normally considered to be superimposed on the waviness. Hence a correct estimate of roughness can be obtained only after the waviness is removed. This was generally accomplished by high pass filtering of the signal representing the profile to remove the low frequencies namely, the waviness. In this regard, J. Raja et al [8] have developed digital filters for profilometer signal processing which can substitute the analogue signal processing.

As the bandwidth of measurement instruments increases, it becomes essential to separate surface profile data into meaningful wavelength regimes before numerical characterization. The different wavelength regimes play a key role in critical parts like crankshafts and bearings. Thus, separation of signal into various bandwidths has to be viewed from a functional standpoint as well. Recent trend in outsourcing of manufacturing makes it essential to define surface texture requirements very clearly. This has made it necessary to use filtering techniques to establish the required wavelength regimes before numerical characterization. In addition, meaningful comparison of parameters from different surface texture measuring instruments can only be done if filtering techniques are used to establish identical bandwidths. Correspondingly, J. Raja et al [8] have reviewed several filters such as 2RC, Gaussian and several new ones currently under research such as the spline, morphological, wavelets, regression filters and robust regression filters. Many attempts were made on the solutions to surface roughness evaluation problems using machine vision system [9] [10]. But, none of them have focused on the estimation of surface roughness of the component after filtering the waviness profile from primary profile in the grey scale images of the components. Besides, while determining the GLCM statistical parameters, the influence of component orientation in the horizontal plane was not considered. In view of this, the present work focuses on the influence of digital filtering of images on the roughness evaluation particularly when using the machine vision approach and the influence of component orientation on image characteristics derived based on GLCM.

## 2. METHODOLOGY

### *2.1 Design of Experiments*

Using the L 9 orthogonal array based design of experiments, number of experiments and the machining parameters were planned. CNC milling operation was performed on flat low carbon steel specimens using tungsten carbide cutting tool. $R_a$ values were obtained from the surface profiles traced using Perthometer with cut-off ($\lambda_c$) values of 0.25, 0.80 and 2.50 mm. Gaussian analogue filter was used in the stylus instrument to filter the waviness profile.

### *2.2 Experimental setup*

The experimental setup as shown in Figure 1 indicates a machine vision system. The gray scale images of the milled components were grabbed by the vision system which is a combination of a lens and a monochrome CCD camera whose pixel array is 1392 X 1040 pixels. Coaxial lighting condition was used and images were grabbed at different locations on each work piece using 4X lens. In addition, the work pieces were oriented at angles of 0, 45and 90 degrees and images at a marked location on each work piece were grabbed. These images were cropped to 512 X 512 pixel size as shown in Figure 2.

Table 1: Machining conditions used and the corresponding roughness parameters

| Speed (rpm) | Feed rate (mm/min) | Depth of cut (µm) | $R_a$ ( µm) ($\lambda_c$=0.25 mm) | $R_a$( µm) ($\lambda_c$=0.8 mm) | $R_a$( µm) ($\lambda_c$=2.5 mm) |
|---|---|---|---|---|---|
| 500 | 50 | 100 | 2.2930 | 5.6097 | 7.5127 |
| 500 | 100 | 200 | 2.1027 | 4.7877 | 5.6533 |
| 500 | 150 | 300 | 1.6033 | 3.4730 | 5.9233 |
| 1000 | 50 | 200 | 0.6683 | 0.7167 | 2.3543 |
| 1000 | 100 | 300 | 0.6260 | 0.9127 | 0.9663 |
| 1000 | 150 | 100 | 0.6367 | 0.8387 | 1.0613 |
| 1600 | 50 | 300 | 0.5673 | 0.6897 | 0.7627 |
| 1600 | 100 | 100 | 1.2943 | 2.0157 | 2.4743 |
| 1600 | 150 | 200 | 1.1263 | 1.7427 | 1.9113 |

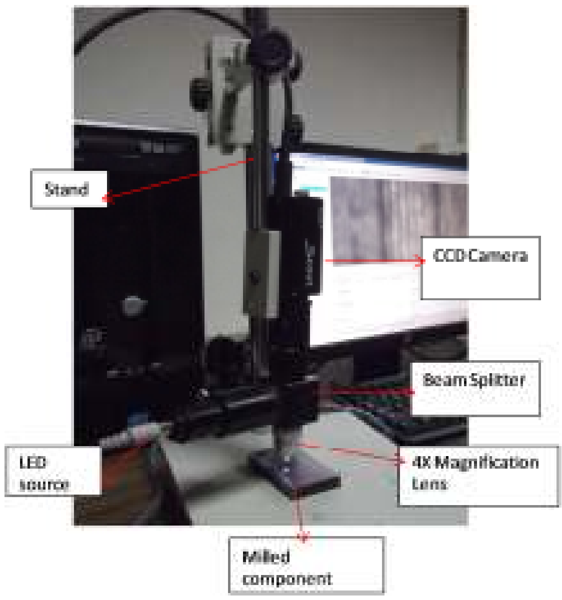


Figure 1: Experimental Setup showing the image capturing

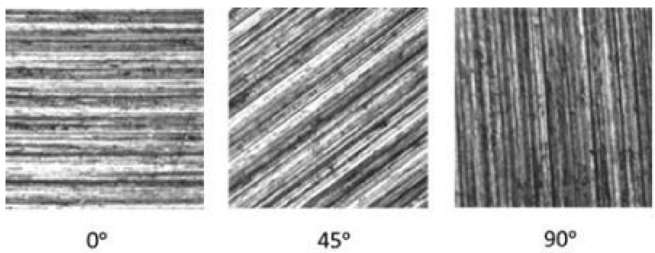


Figure 2: Images captured at 0º, 45 º and 90 º orientation of component

### *2.3 Digital Filtering of the Captured Images*

When the image of a component is captured after it is milled, roughness is superimposed on waviness profile. Many filtering techniques for the waviness profile separation from roughness profile using machine vision have been developed over the past few years. The effect of Butterworth, Gaussian frequency and Mean Gaussian filters on the relationship between $G_a$ and $R_a$ has been analyzed in this work by applying these filters to the Fast Fourier

Transformed images of the components at varied cut-off values and determining the corresponding correlation coefficient between $G_a$ and $R_a$. The Fourier Transform is an important image processing tool which is used to decompose an image into its sine and cosine components. The output of the transformation represents the image in the *Fourier* or frequency domain, while the input image is the spatial domain equivalent. Frequency filters process an image in the frequency domain. The image is Fourier transformed, multiplied with the filter function and then re-transformed into the spatial domain. Attenuating high frequencies results in a smoother image in the spatial domain, attenuating low frequencies enhances the edges.

### *2.3.1 Gaussian Filters*

The Gaussian smoothing operator is a 2-D convolution operator that is used to 'blur' images and remove detail and noise. It uses a kernel that represents the shape of a Gaussian ('bell-shaped') hump. The Gaussian distribution in 1-D has the form:

$$G(x)= \frac{1}{\sqrt{2\pi}\sigma} e^{-\frac{x^2}{2\sigma^2}} \quad (1)$$

where 'σ' is the standard deviation of the distribution. We have also assumed that the distribution has a mean of zero (*i.e.* it is centered on the line *x*=0).

In 2-D, an isotropic (*i.e.* circularly symmetric) Gaussian has the form:

$$G(x)= \frac{1}{\sqrt{2\pi}\sigma} e^{-\frac{x^2+y^2}{2\sigma^2}} \quad (2)$$

The idea of Gaussian smoothing is to use this 2-D distribution as a `point-spread' function, and this is achieved by convolution. Since the image is stored as a collection of discrete pixels it is needed to produce a discrete approximation to the Gaussian function before we can perform the convolution. In theory, the Gaussian distribution is non-zero everywhere, which would require an infinitely large convolution kernel, but in practice it is effectively zero more than about three standard deviations from the mean, and so we can truncate the kernel at this point. Once a suitable kernel has been calculated, then the Gaussian smoothing can be performed using standard convolution methods.

### *2.3.2 Butterworth filter*

A commonly used discrete approximation to the Gaussian is the Butterworth filter. Applying this filter in the frequency domain shows a similar result to the Gaussian smoothing in the spatial domain. One difference is that the computational cost of the spatial filter increases with the standard deviation (*i.e.* with the size of the filter kernel), whereas the costs for a frequency filter are independent of the filter function. Hence, the spatial $G_a$ussian filter is more appropriate for narrow low pass filters, while the Butterworth filter is a better implementation for wide low pass filters. The Butterworth filter is a type of signal processing filter designed to have as flat a frequency response as possible in the pass band. Filters in this class are specified by two parameters, the cut off frequency and the filter order.

The transfer function of a Butterworth low pass filter of order *n* with cut off frequency at distance $D_0$ from the origin for an image with M X N pixels is defined as:

$$H(u,v) = \frac{1}{1+[D(u,v)/Do]^2} \quad (3)$$

$$D(u,v) = \left[\left(u - M/_2\right)^2 + \left(v - N/_2\right)^2\right]^{\frac{1}{2}} \quad (4)$$

Gaussian frequency filter is one form of Gaussian low pass filter. Its transfer function is given by

$$H(u,v) = e^{\frac{-D^2(u,v)}{2Do^2}} \quad (5)$$

## 3. TEXTURE ANALYSIS

Texture analysis refers to the characterization of regions in an image by their texture content. Texture analysis attempts to quantify intuitive qualities described by terms such as rough, smooth, silky, or bumpy as a function of the spatial variation in pixel intensities. In this sense, the roughness or bumpiness refers to variations in the intensity values, or gray levels.

### *3.1 Grey Level Co-occurrence Matrix (GLCM)*

A statistical method of examining texture that considers the spatial relationship of pixels is the grey-level co-occurrence matrix (GLCM). The GLCM functions characterize the texture of an image by calculating how often pairs of pixel with specific values and in a specified spatial relationship occur in an image, creating a GLCM, and then extracting statistical measures from this matrix. The image quantification parameters that can be derived using the inbuilt GLCM tool in MATLAB are as follows:

$$\text{Contrast} = \sum_i \sum_j \left[|i-j|^2 p(i,j)\right] \quad (6)$$

$$\text{correlation}= \sum_i \sum_j \left[\frac{(i-\mu_i)(j-\mu_j)p(i,j)}{\sigma_i \sigma_j}\right] \quad (7)$$

$$\text{energy}= \sum_i \sum_j [p(i,j)]^2 \quad (8)$$

where i and j are the pixel intensities of adjacent pixels and *p( i, j )* is the normalized GLCM of image *N( i, j )*.

The above mentioned quantification parameters were determined for images of the components oriented in different directions in the 2-D plane.

### *3.2 Grey level average* ($G_a$)

This statistical parameter is proposed by Younis and further used by many researchers for quantification of surface roughness of the machined surfaces using machine vision. The arithmetic average of the grey level ($G_a$) can be expressed as

$$Ga = \frac{1}{N_x N_y} \sum_{i=1}^{N_x} \sum_{j=1}^{N_y} |M(i,j)| \quad (10)$$

where $M(i,j)$ is the grey level of the image of the milled component deviated from the mean value and $N_x \times N_y$ represents the size of the image. In the present study, $G_a$ is calculated for the whole image under consideration.

## 4. RESULTS AND DISCUSSIONS

The average surface roughness $R_a$ has been calculated for all the milled components using Perthometer. The grey level average $G_a$ is computed for both filtered and non filtered images and the corresponding correlation coefficients with $R_a$ are compared. The variations of correlation coefficient with filter cut-off are presented. The second order statistical texture parameters based on GLCM are calculated for images of the components captured at varying orientations in 2-D plane. The results thus obtained were compared with those obtained for varying orientations of the components images**.**

### *4.1 Digital filtering*

The $G_a$ values for the images of the milled components captured using 4x magnification at $0^o$ orientation are evaluated before and after filtering and the corresponding correlations with $R_a$ are established as below.

#### *4.1.1 $G_a$ evaluation without filtering*

Table 2: $G_a$ measured for non-filtered milled images and $R_a$ for three different stylus cut-offs

| *sample* | *$G_a$ values without filtering* | *$R_a$ ( $\mu m$) ($\lambda_c$ =0.25 mm)* | *$R_a$ ( $\mu m$) ($\lambda_c$=0.8 mm)* | *$R_a$ ( $\mu m$) ($\lambda_c$=2.5 mm)* |
|---|---|---|---|---|
| 1 | 4.3336 | 2.2930 | 5.6097 | 7.5127 |
| 2 | 5.0630 | 2.1027 | 4.7877 | 5.6533 |
| 3 | 5.3689 | 1.6033 | 3.4730 | 5.9233 |
| 4 | 14.9608 | 0.6683 | 0.7167 | 2.3543 |
| 5 | 17.5089 | 0.6260 | 0.9127 | 0.9663 |
| 6 | 17.4018 | 0.6367 | 0.8387 | 1.0613 |
| 7 | 9.3203 | 0.5673 | 0.6897 | 0.7627 |
| 8 | 10.2333 | 1.2943 | 2.0157 | 2.4743 |
| 9 | 9.4498 | 1.1263 | 1.7427 | 1.9113 |

A maximum correlation coefficient of 0.8685 between $R_a$ and $G_a$ was observed in the case of $\lambda_c$ = 2.5mm stylus cut-off.

#### *4.1.2 $G_a$ evaluation after applying Butterworth filter*:

The cut-off radius of the Butterworth filter was varied from 0.01 to 0.5 in steps of 0.01 and the filter order was maintained constant at a value of 3. $G_a$ values (shown in Table 3) and the correlation factor were determined for the corresponding cut-offs. The best correlation coefficient of 0.938 between $R_a$ and $G_a$ using Butterworth filter was obtained at a cut-off value of 0.05 and stylus cut-off of 25mm λc.

#### *4.1.3: $G_a$ evaluation after applying Gaussian frequency filter*

The cut-off radius of the Gaussian frequency filter was varied, $G_a$ (shown in Table 4) values and the correlation factor were determined for the corresponding cut-offs. The best correlation of 0.9347 between $R_a$ and $G_a$ using this filter was obtained at a cut-off value of 0.04 and stylus cut-off of 25mm $\lambda_c$.

Table 3: $G_a$ measured for images filtered using Butterworth filter cut-off of 0.05 and Ra for three different stylus cut-offs

| *Sample* | *$G_a$ values after applying Butterworth filter* | *$R_a$ ( $\mu m$) ($\lambda_c$=0.25mm)* | *$R_a$ ( $\mu m$) ($\lambda_c$=0.80mm)* | *$R_a$ ( $\mu m$) ($\lambda_c$=2.5 mm)* |
|---|---|---|---|---|
| 1 | 12.7040 | 2.2930 | 5.6097 | 7.5127 |
| 2 | 13.9934 | 2.1027 | 4.7877 | 5.6533 |
| 3 | 13.4989 | 1.6033 | 3.4730 | 5.9233 |
| 4 | 14.1173 | 0.6683 | 0.7167 | 2.3543 |
| 5 | 13.7385 | 0.6260 | 0.9127 | 0.9663 |
| 6 | 11.8929 | 0.6367 | 0.8387 | 1.0613 |
| 7 | 11.2042 | 0.5673 | 0.6897 | 0.7627 |
| 8 | 10.9479 | 1.2943 | 2.0157 | 2.4743 |
| 9 | 13.6094 | 1.1263 | 1.7427 | 1.9113 |

Table 4: $G_a$ measured for images filtered using Gaussian frequency filter and Ra for three different stylus cut-offs

| *sample* | *$G_a$ values after applying Gaussian frequency filter* | *$R_a$ ( $\mu m$) ($\lambda_c$=0.25 mm)* | *$R_a$ ( $\mu m$) ($\lambda_c$=0.8 mm)* | *$R_a$ ( $\mu m$) ($\lambda_c$=2.5 mm)* |
|---|---|---|---|---|
| 1 | 12.02742 | 2.2930 | 5.6097 | 7.5127 |
| 2 | 13.47104 | 2.1027 | 4.7877 | 5.6533 |
| 3 | 13.02666 | 1.6033 | 3.4730 | 5.9233 |
| 4 | 13.06238 | 0.6683 | 0.7167 | 2.3543 |
| 5 | 12.90285 | 0.6260 | 0.9127 | 0.9663 |
| 6 | 11.62454 | 0.6367 | 0.8387 | 1.0613 |
| 7 | 10.5998 | 0.5673 | 0.6897 | 0.7627 |
| 8 | 9.74903 | 1.2943 | 2.0157 | 2.4743 |
| 9 | 13.20673 | 1.1263 | 1.7427 | 1.9113 |

#### *4.1.4: $G_a$ evaluation after applying Mean Gaussian filter*

The cut-off radius of the Mean Gaussian filter was varied and $G_a$ values (shown in Table 5) and the correlation factor were determined for the corresponding cut-offs.

The best correlation of 0.9235 between $R_a$ and $G_a$ using this filter was obtained at a cut-off value of 2.56 and stylus cut-off of 25mm $\lambda_c$

### *4.2: Texture Analysis*

The image quantification parameters were evaluated based on second order statistical method GLCM for images of the milled component captured in varying orientations of the component. The results thus obtained are presented in Tables 6, 7 and 8 respectively.

Table 5: $G_a$ measured for images filtered using Mean Gaussian filter and $R_a$ for three different stylus cut-offs

| *sample* | *$G_a$ values after applying mean Gaussian filter* | *$R_a$ ( μm)* (λc=0.25 mm) | *$R_a$ ( μm)* (λc=0.8 mm) | *$R_a$ ( μm)* (λc=2.5 mm) |
|---|---|---|---|---|
| 1 | 15.69333 | 2.2930 | 5.6097 | 7.5127 |
| 2 | 16.63218 | 2.1027 | 4.7877 | 5.6533 |
| 3 | 17.55343 | 1.6033 | 3.4730 | 5.9233 |
| 4 | 18.05989 | 0.6683 | 0.7167 | 2.3543 |
| 5 | 16.9156 | 0.6260 | 0.9127 | 0.9663 |
| 6 | 15.19334 | 0.6367 | 0.8387 | 1.0613 |
| 7 | 15.09933 | 0.5673 | 0.6897 | 0.7627 |
| 8 | 15.09159 | 1.2943 | 2.0157 | 2.4743 |
| 9 | 17.39721 | 1.1263 | 1.7427 | 1.9113 |

### *4.2.1 Contrast*

In the texture analysis of the images, the image quantification parameter contrast varied with orientations of the components. For 90° there is a minimum contrast in the images as lay direction is almost parallel to the y-axis in this orientation and the pixel intensities are compared with their neighboring pixels which lie to the immediate above the original pixel along the y-axis.

Table 6: Contrast measured for Butterworth filtered images for varied orientations of the components in the 2D plane

| | *GLCM Contrast* | | |
|---|---|---|---|
| *Sample* | 0° | 45° | 90° |
| 1 | 90.69 | 93.97 | 59.09 |
| 2 | 122.23 | 104.46 | 86.96 |
| 3 | 130.08 | 81.85 | 65.02 |
| 4 | 590.98 | 375.67 | 86.79 |
| 5 | 715.09 | 214.81 | 45.66 |
| 6 | 716.14 | 528.50 | 92.19 |
| 7 | 336.48 | 173.40 | 65.87 |
| 8 | 317.66 | 161.55 | 59.88 |
| 9 | 293.30 | 199.67 | 84.35 |
| *Correlation coefficient (r)* | 0.81 | 0.65 | 0.11 |

Since the pixel intensities along the lay direction do not vary much, not much contrast is observed between adjacent pixels due to which the overall contrast of the image is less. The correlation between image contrast and $R_a$ for the nine components was the least for 90° orientation of the component image and the highest for 0° orientation.

### *4.2.2 Image correlation*

The image correlation values are the highest for 90°component image orientation. This is because, along the lay direction pixels have almost same intensity values and hence each pixel is well correlated with its neighbouring pixel.

Table 7: Correlation measured for Butterworth filtered images for varied orientations of the components in the 2D plane

| | *GLCM Correlation* | | |
|---|---|---|---|
| *Sample* | 0° | 45° | 90° |
| 1 | 0.5749 | 0.6681 | 0.7857 |
| 2 | 0.6363 | 0.7081 | 0.7625 |
| 3 | 0.5986 | 0.7552 | 0.8178 |
| 4 | 0.5152 | 0.6563 | 0.8656 |
| 5 | 0.4845 | 0.7227 | 0.8994 |
| 6 | 0.5073 | 0.6358 | 0.9118 |
| 7 | 0.5732 | 0.7400 | 0.8794 |
| 8 | 0.6147 | 0.7138 | 0.8361 |
| 9 | 0.5919 | 0.7157 | 0.8418 |
| *Correlation coefficient (r)* | 0.58 | 0.04 | 0.91 |

The correlation between pixel correlation and $R_a$ for the nine components was the least for 45° orientation of the component image and the highest for 90° orientation.

### *4.2.3 Energy or Uniformity*

Table 8: Energy measured for Butterworth filtered images for varied orientations of the components in the 2D plane

| | *GLCM Energy* | | |
|---|---|---|---|
| *Sample* | 0° | 45° | 90° |
| 1 | 0.00461 | 0.00336 | 0.00320 |
| 2 | 0.00225 | 0.00229 | 0.00214 |
| 3 | 0.00289 | 0.00220 | 0.00266 |
| 4 | 0.00037 | 0.00042 | 0.00106 |
| 5 | 0.00032 | 0.00066 | 0.00167 |
| 6 | 0.00030 | 0.00032 | 0.00082 |
| 7 | 0.00076 | 0.00090 | 0.00148 |
| 8 | 0.00071 | 0.00123 | 0.00215 |
| 9 | 0.00082 | 0.00076 | 0.00133 |
| *Correlation coefficient (r)* | 0.95 | 0.97 | 0.87 |

The correlation between image uniformity and $R_a$ for the nine components was the least for 0.87° orientation of the component image and the highest for 45°orientation.

## 5 CONCLUSIONS

Experiments have been carried out using the CNC milling process and the milled components have been measured for the surface roughness using stylus instrument produced with different machining parameters. Using this as a basis, images of the components were captured when they were stationary in varying angular orientations in the 2-D plane. Using these images vision roughness parameters were calculated and compared with the stylus roughness values. Linear regression analysis was used to establish the correlation between $G_a$ and $R_a$. The images captured were filtered using Gaussian and Butterworth low pass filters in the frequency domain and $G_a$ values were re-determined and then the comparison was done.

Vision roughness values were observed to correlate well with the stylus roughness values obtained using 2.5mm $\lambda_c$ filter cut-off in the stylus instrument and for the images captured in 0º orientation of the components for GLCM contrast and GLCM Correlation.

Vision roughness values of the components after digital filtering of the images were found to be in better correlation with the stylus roughness values than those obtained without filtering.

## REFERENCES


[1] Sodhi, Manbir S., and Khalil Tiliouine. "Surface roughness monitoring using computer vision." *International Journal of Machine Tools and Manufacture* 36.7 (1996): 817-828.

[2] Priya, P., and B. Ramamoorthy. "The influence of component inclination on surface finish evaluation using digital image processing." *International Journal of Machine tools and manufacture* 47.3 (2007): 570-579.

[3] Whitehouse, David J. *Surfaces and their Measurement*. Butterworth-Heinemann, 2004.

[4] Damodarasamy, Sampath, and Shivakumar Raman. "Texture analysis using computer vision." *Computers in industry* 16.1 (1991): 25-34.

[5] Venkat Ramana, K., and B. Ramamoorthy. "Statistical methods to compare the texture features of machined surfaces." *Pattern Recognition* 29.9 (1996): 1447-1459.

[6] Haralick, Robert M., Karthikeyan Shanmugam, and Its' Hak Dinstein. "Textural features for image classification." *Systems, Man and Cybernetics, IEEE Transactions on* 6 (1973): 610-621.

[7] Gadelmawla, E. S. "A vision system for surface roughness characterization using the gray level co-occurrence matrix." *NDT & E International* 37.7 (2004): 577-588.

[8] Raja, J., B. Muralikrishnan, and Shengyu Fu. "Recent advances in separation of roughness, waviness and form." *Precision Engineering* 26.2 (2002): 222-235.

[9] Yuan, Y. B., W. Y. Piao, and J. B. Xu. "A fast Gaussian filtering algorithm for three-dimensional surface roughness measurements." *Journal of Physics: Conference Series*. Vol. 48. No. 1. IOP Publishing, 2007.

[10] Yuan, Y. B., et al. "A simplified realization for the Gaussian filter in surface metrology." *International Colloquium on Surfaces, Chemnitz (Germany), Jan*. 2000.